Direct evidence of the molecular structure of the ground state of the neutron-rich ^{10}Be nucleus

P.J. Li,[1,2,*] D. Beaumel,[3,4,†] J. Lee,[2,‡] M. Assié,[3] S. Chen,[2] S. Franchoo,[3] J. Gibelin,[5] F. Hammache,[3] T. Harada,[4] Y. Kanada-En'yo,[6] Y. Kubota,[4] S. Leblond,[2] P.F. Liang,[2] T. Lokotko,[2] M. Lyu,[7] F. M. Marqués,[5] Y. Matsuda,[8] K. Ogata,[9,10] H. Otsu,[4] E. Rindel,[3] L. Stuhl,[11] D. Suzuki,[4] Y. Togano,[12] T. Tomai,[13] X.X. Xu,[1,2] K. Yoshida,[14] J. Zenihiro,[4] L. Achouri,[5] H. Baba,[4] G. Cardella,[15] S. Ceruti,[16] A. Chilug,[17,18] A. Corsi,[19] A. Frotscher,[20] J. Gao,[21] A. Gillibert,[19] K. Inaba,[22] T. Isobe,[4] T. Kawabata,[23] N.Kitamura,[4] T. Kobayashi,[24] Y. Kondo,[13] A. Kurihara,[13] H.N. Liu,[20] H. Miki,[13] T. Nakamura,[13] A. Obertelli,[20] N. Orr,[5] V. Panin,[4] M. Sasano,[4] T. Shimada,[13] Y.L. Sun,[20] J. Tanaka,[4] L. Trache,[17] D. Tudor,[17,18] T. Uesaka,[4] H. Wang,[4] H. Yamada,[13] Z.H. Yang,[4,21] and M. Yasuda[13]

(SAMURAI12 Collaboration)[§]

[1] *CAS Key Laboratory of High Precision Nuclear Spectroscopy, Institute of Modern Physics, Chinese Academy of Sciences, Lanzhou 730000, China*
[2] *Department of Physics, The University of Hong Kong, Hong Kong, China*
[3] *Université Paris-Saclay, CNRS/IN2P3, IJCLab, 91405 Orsay, France*
[4] *RIKEN Nishina Center, Hirosawa 2-1, Wako, Saitama 351-0198, Japan*
[5] *LPC Caen, ENSICAEN, Université de Caen, CNRS/IN2P3, F-14050 CAEN Cedex, France*
[6] *Department of Physics, Kyoto University, Kyoto 606-8502, Japan*
[7] *College of Physics, Nanjing University of Aeronautics and Astronautics, Nanjing 210016, China*
[8] *Cyclotron and Radioisotope Center, Tohoku University, Sendai 980-8578, Japan*
[9] *Department of Physics, Kyushu University, Fukuoka 819-0395, Japan*
[10] *Research Center for Nuclear Physics (RCNP), Osaka University, Ibaraki 567-0047, Japan*
[11] *Center for Nuclear Study, University of Tokyo, RIKEN campus, Wako, Saitama 351-0198, Japan*
[12] *Department of Physics, Rikkyo University, 3-34-1 Nishi-Ikebukuro, Toshima, Tokyo 172-8501, Japan*
[13] *Department of Physics, Tokyo Institute of Technology, 2-12-1 O-Okayama, Meguro, Tokyo 152-8551, Japan*
[14] *Advanced Science Research Center, Japan Atomic Energy Agency, Tokai, Ibaraki 319-1195, Japan*
[15] *Istituto Nazionale di Fisica Nucleare, Sezione di Catania, Italy*
[16] *INFN Sezione di Milano, 20133, Milano, Italy*
[17] *Horia Hulubei National Institute for R&D in Physics and Nuclear Engineering (IFIN-HH), Romania*
[18] *Doctoral School of Physics - University of Bucharest, Magurele, Romania*
[19] *IRFU, CEA, Université Paris-Saclay, F-91191 Gif-sur-Yvette, France*
[20] *Institut für Kernphysik, Technische Universität Darmstadt, D-64289 Darmstadt, Germany*
[21] *School of Physics and State Key Laboratory of Nuclear Physics and Technology, Peking University, Beijing 100871, China*
[22] *Department of Physics, Kyoto University, Kitashirakawa-Oiwake, Sakyo, Kyoto 606-8502, Japan*
[23] *Department of Physics, Osaka University, Toyonaka, Osaka 540-0043, Japan*
[24] *Department of Physics, Tohoku University, Sendai 980-8578, Japan*

(Dated: November 18, 2022)

The cluster structure of the neutron-rich isotope ^{10}Be has been probed via the $(p, p\alpha)$ reaction at 150 MeV/u in inverse kinematics and in quasifree conditions. The populated states of ^{6}He were investigated through missing mass spectroscopy. The triple differential cross-section for the ground-state transition was extracted for quasifree angle pairs (θ_p, θ_α) and compared to distorted-wave impulse approximation reaction calculations performed in a microscopic framework using successively the Tohsaki-Horiuchi-Schuck-Röpke product wave-function and the wave-function deduced from Antisymmetrized Molecular Dynamics calculations. The remarkable agreement between calculated and measured cross-sections in both shape and magnitude validates the description of the ^{10}Be ground-state as a rather compact nuclear molecule.

Introduction The formation of structures in nuclei that have large scale clustering is an intriguing phenomenon and is in part driven by correlations which stem from the details of the nucleon-nucleon interaction. Among the different partitioning possibilities within a given nucleus, alpha clustering has always been considered the most favorable due to the large binding energy of the alpha particle and its inert character. Therefore, nuclei composed of an integer number of alpha particles (the so-called self-conjugate nuclei) initially focused clustering studies. The Ikeda diagram [1], which appeared at the end of the 1960s, conveys the idea that the cluster degrees of freedom appear in the vicinity of the alpha emission thresholds, the energy for which the nucleus can dissociate into an alpha particle and a residue. The famous Hoyle state, the second 0+ state of ^{12}C which plays a key-role in the nucleosynthesis of elements heavier than helium is a typical example of such a cluster state. It is

located at an energy just above the three-alpha threshold in ^{12}C. Its basic structure in three alphas is established, but its nature is still an object of study. For example, this state can be described as a condensate of alpha particles occupying a large volume using a wave function of Tohsaki-Horiuchi-Schuck-Roepke (THSR) type [2]. Calculations in the antisymmetrized molecular dynamics (AMD) approach confirm the significant spatial extension of this state and suggest a structure dominated by a "loose" configuration in ^{8}Be+alpha[3]. In contrast, the ground state of ^{12}C is described in the above models as rather compact, with mean-field like structure, in accordance with the idea of the Ikeda diagram for self-conjugate nuclei.

As compared to self-conjugate nuclei, the situation is different in neutron-rich light nuclei. For example, strong indications exist that in low-lying states of Be and B isotopes, including the ground-state, adding neutrons to an $N = Z$ core leads to spatially extended molecular-like structures in which valence neutrons orbit around the core composed of alpha particles. A typical case is represented by the neutron-rich ($N > 4$) beryllium isotopes which were initially described as systems of two alpha + Xn, the two alphas exhibiting a dumbbell shape core in the intrinsic frame and X being the number of excess neutrons occupying molecular orbitals around this core[4]. The ground state of ^{9}Be, the only stable beryllium isotope, may be described as a 3-body $\alpha - n - \alpha$ molecular structure. Experimentally, The ^{9}Be ground-state rotational band is well understood in terms of π orbital, while the band observed for the first ($\frac{1}{2}$+) excited state at 1.68 MeV can be connected to a σ-type molecular structure. This description of the cluster structure initially elaborated in molecular orbital models was later confirmed by mean-field type approaches, namely AMD, from which the cluster structures emerge without the existence of clusters being presupposed. The next neutron-rich Be isotope is ^{10}Be, an unstable nucleus which structure i is also expected to exhibit a marked molecular character. Experimental studies of this nucleus have revealed four rotational bands, corresponding to various cluster structures for excited states. However, little is known about the cluster structure of its ground state, apart from the rotational band built on the ground state. The charge radius, which can be measured precisely, is directly related to the density distribution of protons, though not probing directly the cluster structure of ground-states. Among the beryllium isotopes, ^{10}Be exhibits the smallest charge radius, which is consistent with AMD calculations that predict a minimum for N=6[5]. In these calculations, the ground state of ^{10}Be is described as a two alpha + two neutron configuration, in which valence neutron occupy the molecular attractive π orbital which produces a more compact 2-alpha core, at variance with σ orbitals [6]. It should be noted that this configuration is also predicted in Density Functional Theory (DFT) calculations [7] a general framework within which a large number of properties of nuclei can be reproduced. Namely, the dumbbell shape structure of the alphas as well as the ring-type orbits of the neutrons emerge from the mean-field.

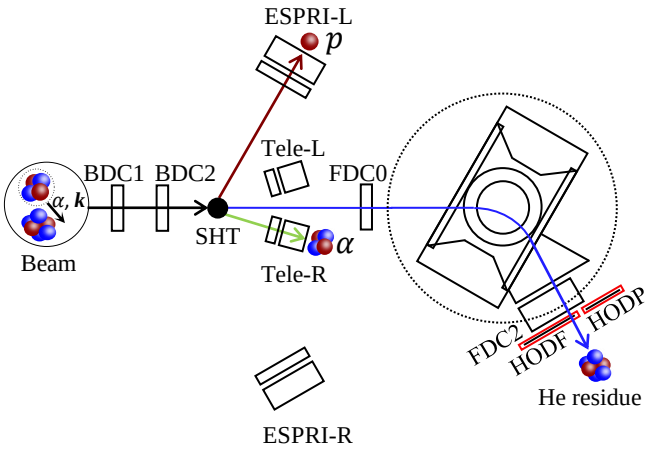

FIG. 1. Schematic view of ^{10}Be$(p, p\alpha)^{6}$He reaction setup.

The important point for our purpose is that for neutron-rich Beryllium isotopes, the occupancy of molecular orbitals by valence neutrons is strongly correlated with the spatial extension of the alpha wave-function. In order to directly probe the spatial extension of alpha clusters in the ground state of ^{10}Be and thus establish its cluster structure, we implemented a method based on cluster knockout reactions of the $(p, p\alpha)$ type. These reactions have been studied extensively with proton beams on stable targets in the 80's and until today. Until recently, it is essentially the alpha spectroscopic factors that were extracted from these measurements. These spectroscopic factors are integrated quantities that do not give direct information about the spatial distribution of alphas in the nucleus. In the present work we have: 1. Performed for the first time the measurement of the triple differential cross-section (TDX) of the $(p, p\alpha)$ reaction in inverse kinematics using a beam of unstable nuclei of ^{10}Be and in kinematical conditions covering the recoilless condition and 2. Compared the measured TDX to reaction calculations carried out in a microscopic framework, including in particular the microscopic cluster wave function. In a previous work, the sensitivity of the TDX observable to the alpha wave function hence to the geometric configuration of the alpha clusters in the ground-state of ^{10}Be was demonstrated[8]. In particular, it was shown that the magnitude of the TDX is strongly correlated with the intercluster distance which is key to infer the overall structure of the ^{10}Be ground-state, as mentioned above.

Experiment The experiment was performed at the Radioactive Isotope Beam Factory (RIBF) of the RIKEN Nishina Center. A secondary beam of ^{10}Be was produced at an energy of approximately 150 MeV/nucleon through

projectile fragmentation of a 230 MeV/nucleon ^{18}O beam impinging on a 15-mm-thick Be target and purified using the BigRIPS fragment separator[9]. The average ^{18}O beam intensity was 500 pnA and the produced ^{10}Be beam intensity was of 5×10^5 particles with a purity higher than 90%. ^{10}Be beam particles were identified on an event-by-event basis. Figure 1 shows the main components of the experimental setup around the secondary target. Beam ions were tracked by a set of two multiwire drift chambers(MWDC) placed upstream of the target chamber. To minimize multiple scattering of recoil protons from the ^{10}Be$(p,p\alpha)$ reaction in inverse kinematics, a 2mm-thick pure solid hydrogen target (SHT)[10] was used as the reaction target. Recoil protons were detected using the Recoil Proton Spectrometer (RPS) described in[11, 12] in a two-arm configuration set at 60° with respect to the beam axis. Each arm was composed of three stages (MWDC, plastic scintillator and NaI(Tl) rods) providing position and energy measurement which were used to reconstruct the scattering angle and total energy of the recoil protons. Given the energy range of the recoil protons for the reaction of interest in the present measurement (25-100 MeV), data from the elastic and inelastic channels were used to perform the energy calibration of RPS. Knocked-out α-clusters were measured by two telescopes composed of double-sided strip Silicon detector (DSSD) of 62×62 mm^2 active surface backed by CsI(Tl) modules from the FARCOS array [13] placed in the horizontal plane to cover the angular range 4° - 12°. The identification of Helium residues emitted around zero degrees was performed using the SAMURAI spectrometer and its standard plastic hodoscopes [14].

Results Fig.2 displays the excitation energy spectra in ^{6}He for the ^{10}Be$(p,p\alpha)$ reaction obtained from the measured energy and angle of both the recoil proton and alpha cluster. The present triple coincidence measurement produces spectra with rather low background. The GS being the only bound state in ^{6}He, the GS→GS transition is easily separated by setting a gate on the ^{6}He residues in SAMURAI. The corresponding peak (red histogram) is well fitted by a Gaussian positioned at (-0.02 ± 0.03) MeV with a missing mass resolution of $\sigma = 1.06$ MeV. The spectrum gated by ^{4}He residues corresponds to the excited states populated in the ^{10}Be$(p,p\alpha)^6$He* $\rightarrow^4$He+$2n$ reaction channel. The resolution does not allow a clear identification of the populated states. For the spectrum of Fig.2(b) a fit was performed including the well-known 2^+ state located at 1.797 MeV[15] and other low-lying resonant states found in the 2-6 MeV region according to [15–19]. The present spectrum is well reproduced by a combination of the 2^+ state, a resonance at around 3.5 MeV observed in [19] and predicted by theoretical calculations as the 2^+_2 state [20, 21], and a third resonance observed at 7.3 MeV in several experiments.

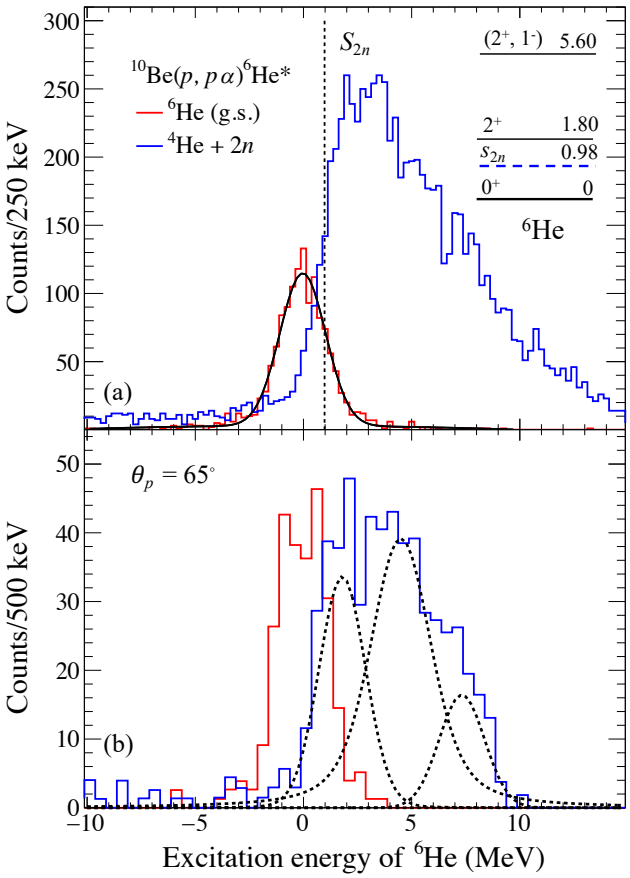

FIG. 2. Excitation energy spectra for ^{10}Be$(p,p\alpha)^6$He* reaction. (a) integrated over the full solid angle covered by proton and cluster detectors. The vertical dashed line indicates the 2-neutron separation energy(0.975 MeV). The red and blue solid lines show spectra corresponding to events gated by ^{6}He and ^{4}He residues, respectively. (b) same for events corresponding to the quasifree angle pair ($\theta_p/\theta_\alpha = 65^\circ/-7.7^\circ$) with an angular bin size of ±1°.

Cross-sections The experimental TDX for the $(p,p\alpha)$ reaction were extracted for the coplanar angle pairs (θ_p,θ_α) chosen to include zero recoil momentum condition of the residual nucleus. The experimental TDX is given in the unit of μb/(sr^2·MeV) in the laboratory system. For a given angle pair (θ_p,θ_α), the TDX for a given transition can be written as:

$$\frac{d^3\sigma^{exp}}{dT_p d\Omega_p d\Omega_\alpha} = \frac{\Delta N(T_p)}{\varepsilon_d N_t N_b \Delta T_p \cdot \varepsilon_{\varphi_p}(\theta_p)\varepsilon_{\varphi_{p\alpha}}(\varphi_p) PV(T_p)} \quad (1)$$

where index p and α stand for the outgoing proton and alpha, respectively; $\Delta N(T_p)$ is the number of counts in an energy bin ΔT_p; ε_d is the "intrinsic" detection efficiency of proton and alpha detectors; N_t is the number of proton per unit area of the SHT; N_b is the number of incident beam particles; $\varepsilon_{\varphi_p}(\theta_p)$ is the φ_p acceptance at θ_p obtained from the simulation; $\varepsilon_{\varphi_{p\alpha}}(\varphi_p)$ is the efficiency of detecting a p-α pair at φ_p obtained from the

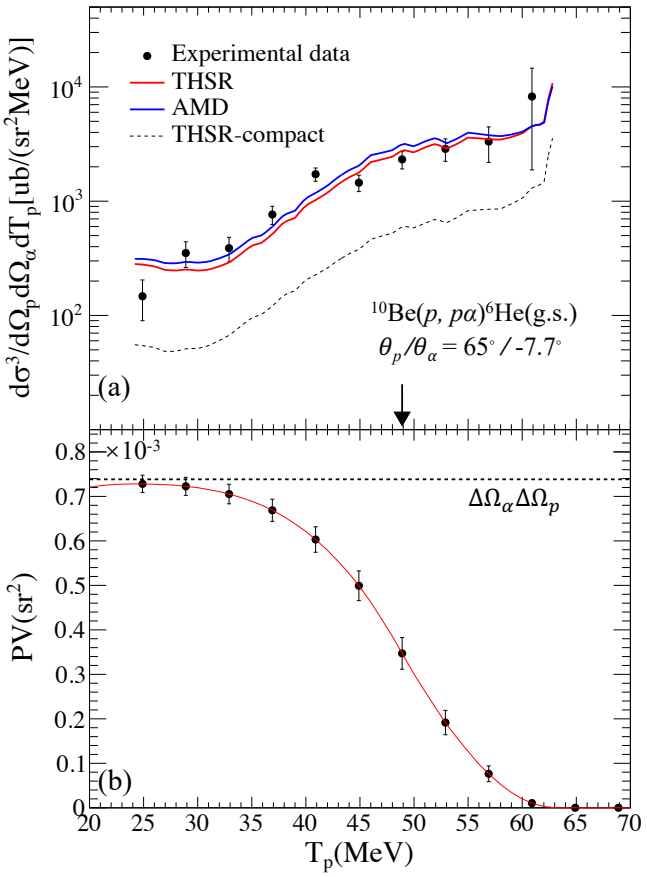

FIG. 3. (a) TDX distribution of of ^{10}Be$(p, p\alpha)^6$He(g.s.) reaction extracted at the coplanar angle pairs $\theta_p/\theta_\alpha = 65°/-7.7°$ which were chosen to include zero recoil momentum condition of the residual nucleus.The arrow indicates T$_p$ at the quasifree condition. The solid line represents DWIA calculations; (b) The corresponding phase volume distribution.

simulation; The phase volume term $PV(T_p)$ corresponding to the portion of the $\Delta\Omega_p \cdot \Delta\Omega_\alpha$ volume kinematically allowed can be defined in discrete form by :

$$PV(T_p) = \sum_{\theta_p}\sum_{\varphi_p}\sum_{\theta_\alpha}\sum_{\varphi_\alpha} \sin\theta_p \Delta\theta_p \Delta\varphi_p \cdot \sin\theta_\alpha \Delta\theta_\alpha \Delta\varphi_\alpha \tag{2}$$

where the summation ranges of θ_p, θ_α, φ_p, and φ_α are restricted to satisfy the energy-momentum conservation.

Fig.3(a) shows the extracted experimental TDX for the ^{10}Be$(p, p\alpha)^6$He(g.s.) reaction at the angle pairs $(\theta_p/\theta_\alpha = 65°/-7.7°)$ compared with the reaction calculations discussed below. The arrow in the plot indicates the T_p corresponding to the recoilless condition. The error bars correspond to the sum of statistical uncertainties and those on the PV induced by the error on the scattering angle. First of all, we note that the shape of the TDX distribution in inverse kinematics is heavily influenced by the PV term in the denominator of Eq. 1. Unlike the case of TDX in forward kinematics for an orbital angular momentum transfer L=0, it is no longer a peak centered at the value of T_p corresponding to the recoilless condition.

Explicit formulae of $(p,p\alpha)$ TDX within the DWIA framework can be found in Eqs. (4)–(7) of Ref. [22]. See Ref. [23–25] for detailed DWIA description.

In Fig.3(a) the experimental TDX is compared to the result of calculations within the DWIA framework using microscopic RWA of the ground state of ^{10}Be obtained by the THSR and AMD models. The structure calculation of ^{10}Be of the THSR model was presented in Ref.[8], and that of the AMD model was presented in Ref.[26]. Both calculations have been performed for an incident energy of 150 AMeV used in the experiment. The proton optical potentials were deduced from the democratic parameterization of Dirac phenomenology [27]. As for the p-α elementary process, p-α differential cross section obtained by the folding model potential [28] using the Melbourne g-matrix interaction[29] is adopted. In both THSR and AMD cases, the RWA used in the calculation has been obtained from the approximation method described in [30]. Fig.3 shows that the shape of the experimental TDX distribution of ^{10}Be$(p, p\alpha)^6$He(g.s.) is very well reproduced by both calculations. Furthermore, the normalization of the calculated distributions to the experimental one by a fitting procedure leads to normalization factors of 1.04(7) and 0.90(6) for the THSR and AMD, respectively, very close to unity. The present microscopic descriptions of the ^{10}Be$(p, p\alpha)^6$He(GS) reaction allow to reproduce the data very well.

TABLE I. Comparison of the experimental and theoretical cross-sections for the ground state and 2^+ excited state transitions at quasifree conditions. Both σ_{exp} and σ_{th} are integrated over the angle bin size of ±1°.

Final state	$[\theta_p/\theta_\alpha]$ (deg)	σ_{exp} (mb/sr^2)	$\sigma_{\rm THSR}$ (mb/sr^2)	$\sigma_{\rm AMD}$ (mb/sr^2)
^{6}He(g.s.)	65°/7.7°	23.6(28)	22.7/5.0	25.9
^{6}He(2^+)	65°/7.5°	16.1(34)	5.2	7.9

Integrated cross sections The population of the excited states as well as the ground state of ^{6}He measures the contribution of He core-excited states in the ground state of ^{10}Be. Table I gives the extracted double differential cross-sections for the ground-state and 2^+ excited-state transitions at the quasifree condition obtained by integrating the TDX over the proton kinetic energy T$_p$. Due to the slight variation of the residue mass, there is a corresponding change in the quasifree angle pairs, while $\theta_p = 65°$ remains unchanged for both cases. The number of counts for the ground state transition is extracted straightforwardly as only the ground state of ^{6}He is bound, while that for the 2^+ excited state transition is obtained through a decomposition of the excitation energy spectrum, as shown in Fig.2. The spectrum was fitted by three resonances modeled as the convolution

of a Breit–Wigner distribution with a Gaussian function, taking into account the experimental resolution. The parameters of the 2^+ resonances (1.797 MeV, Γ = 0.113 MeV) are taken from [15], and the energy E and width Γ of the other two resonances are free parameters, All the normalization parameters are also set free in the fit.

As shown in Table I, the experimental cross-sections are compared with that from DWIA calculations. The calculation of ground-state transition reproduces well the cross-section extracted from the present experimental data; Considering the errors inherent to the excitation energy spectrum decomposition, the calculation of 2^+ excited state transition and the experimental results are also considered consistent.

Discussion The ground-state structure of ^{10}Be within the THSR-based framework described in [8] corresponds to a molecular configuration of two alpha cores with two additional neutrons occupying π orbitals. It is rather pure due to the fact that for Be isotopes, N=6 is a good magic number. This configuration is spatially extended, although to a lower extent than for other beryllium isotopes because of the attractive effect of the π neutrons compared to e.g. neutrons in σ orbits. Consistently, the corresponding root-mean-square charge radius of ^{10}Be is 2.31 fm, very close to the experimental value. The sensitivity of the TDX of the ^{10}Be$(p,p\alpha)^6$He(g.s.) reaction to the spatial extension of the alpha cluster wave-function, quantified by the intercluster distance has been clearly demonstrated in [8], and the present results thus provide a direct validation of the above molecular structure. For comparison, we performed the TDX calculation using the compact shell-model like description (referred as shell model limit in [8]) of the ground-state of ^{10}Be at the incident energy used in the present experiment. Although unphysical, this state allows to test the impact on the TDX magnitude of a compact ground-state in terms of spatial distribution of alpha clusters. As expected, a very large normalization factor is needed to match the magnitude of the data.

The AMD approach has been successfully used for long to describe and establish low-lying molecular structures in light nuclei. This framework is general enough to enable description of both single-nucleon properties as well as cluster structure, without assuming preformed cluster. Within this framework, the ^{10}Be ground-state is found to have a structure as the one inferred with the THSR model wave function in the region of interest. Namely, the RWA have similar behaviour at the surface region which contributes to the cross-section in both models. Consistently, we find that the calculated TDX using AMD RWA shows an agreement of similar quality with the data as when using the THSR approach.

Conclusion The cluster structure of an unstable neutron-rich nucleus, ^{10}Be, has been investigated by measuring for the first time the TDX of the $(p,p\alpha)$ reaction in inverse kinematics with a setup allowing inclusion of the recoilless condition. Double differential cross-sections to the ground and 2+ states of the ^{6}He residue have also been extracted. Obtained data have been compared with cross-section calculations performed within a microscopic DWIA framework involving up-to-date alpha-cluster wave functions, describing the ground-state in terms of a dumbbell-shaped two-alpha core (with moderate extension) surrounded by two neutrons occupying π orbit. A remarkable agreement in both shape and magnitude between the experimental and calculated TDX for the ^{10}Be$(p,p\alpha)^6$He(GS). Due to the previously established sensitivity of the TDX to the extension of the alpha wave-function in the ground-state of ^{10}Be, our results provide direct experimental evidence of the above molecular structure of ^{10}Be implemented in the THSR approach, and validated by the general AMD framework. In the latter, this cluster structure emerges from the details of the nuclear mean field. Concerning the double differential cross-sections to the GS and 2+ states of the residue, a good agreement between calculations and experimental results is found. A consistent picture is then obtained.

* lipengjie@impcas.ac.cn
† beaumel@ipno.in2p3.fr
‡ jleehc@hku.hk
§ A footnote to the article title

[1] K. Ikeda, N. Takigawa, and H. Horiuchi, Progress of Theoretical Physics Supplement **E68**, 464 (1968).
[2] A. Tohsaki, H. Horiuchi, P. Schuck, and G. Röpke, Phys. Rev. Lett. **87**, 192501 (2001).
[3] M. Freer, H. Horiuchi, Y. Kanada-En'yo, D. Lee, and U.-G. Meißner, Rev. Mod. Phys. **90**, 035004 (2018).
[4] W. Von Oertzen, M. Freer, and Y. Kanada-En'yo, Physics Reports **432**, 43 (2006).
[5] Y. Kanada-En'yo, Phys. Rev. C **91**, 014315 (2015).
[6] Y. Kanada-En'yo and H. Horiuchi, Progress of Theoretical Physics Supplement **142**, 205 (2001).
[7] J.-P. Ebran, E. Khan, T. Nikšić, and D. Vretenar, Phys. Rev. C **90**, 054329 (2014).
[8] M. Lyu, K. Yoshida, Y. Kanada-En'yo, and K. Ogata, Phys. Rev. C **97**, 044612 (2018).
[9] T. Kubo, Nucl. Instrum. Methods Phys. Res., Sect. B **204**, 97 (2003).
[10] Y. Matsuda *et al.*, Nucl. Instrum. Methods Phys. Res., Sect. A **643**, 6 (2011).
[11] S. Chebotaryov *et al.*, Prog. Theor. Exp. Phys. **2018** (2018), 053D01.
[12] Y. Matsuda *et al.*, Phys. Rev. C **87**, 034614 (2013).
[13] G. Verde *et al.*, J. Phys.: Conf. Ser. **420**, 012158 (2013).
[14] T. Kobayashi *et al.*, Nucl. Instrum. Methods Phys. Res., Sect. B **317**, 294 (2013).
[15] D. Tilley, C. Cheves, J. Godwin, G. Hale, H. Hofmann, J. Kelley, C. Sheu, and H. Weller, Nucl. Phys. A **708**, 3 (2002).
[16] X. Mougeot *et al.*, Phys. Lett. B **718**, 441 (2012).
[17] H. T. Fortune, Phys. Rev. C **89**, 014326 (2014).

[18] G. Mandaglio *et al.*, Mod. Phys. Lett. A **29**, 1450105 (2014).
[19] Y. B. Gurov *et al.*, Bull. Russ. Acad. Sci. Phys. **79**, 470 (2015).
[20] S. Ogawa and T. Matsumoto, Phys. Rev. C **102**, 021602 (2020).
[21] T. Myo, K. Katō, and K. Ikeda, Phys. Rev. C **76**, 054309 (2007).
[22] K. Yoshida and J. Tanaka, Phys. Rev. C **106**, 014621 (2022).
[23] N. S. Chant and P. G. Roos, Phys. Rev. C **15**, 57 (1977).
[24] N. S. Chant and P. G. Roos, Phys. Rev. C **27**, 1060 (1983).
[25] T. Wakasa, K. Ogata, and T. Noro, Progress in Particle and Nuclear Physics **96**, 32 (2017).
[26] Y. Kanada-En'yo, H. Horiuchi, and A. Doté, Phys. Rev. C **60** (1999).
[27] E. D. Cooper, S. Hama, and B. C. Clark, Phys. Rev. C **80**, 034605 (2009).
[28] M. Toyokawa, K. Minomo, and M. Yahiro, Phys. Rev. C **88**, 054602 (2013).
[29] K. Amos, P. J. Dortmans, H. V. von Geramb, S. Karataglidis, and J. Raynal, Advances in Nuclear Physics **25**, 276 (2000).
[30] Y. Kanada-En'yo, T. Suhara, and Y. Taniguchi, Prog. Theor. Exp. Phys. **2014** (2014), 073D02.